THE JOURNAL OF BIOLOGICAL CHEMISTRY VOL. 282, NO. 43, pp. 31517–31524, October 26, 2007


# A Novel Mechanism for Substrate Inhibition in *Mycobacterium tuberculosis* D-3-Phosphoglycerate Dehydrogenase*

Received for publication, May 16, 2007, and in revised form, August 9, 2007 Published, JBC Papers in Press, August 30, 2007, DOI 10.1074/jbc.M704032200

**Rodney L. Burton‡, Shawei Chen‡, Xiao Lan Xu‡, and Gregory A. Grant‡§1**

*From the Departments of ‡Molecular Biology & Pharmacology and §Medicine, Washington University School of Medicine, St. Louis, Missouri 63110*

***Mycobacterium tuberculosis* D-3-phosphoglycerate dehydrogenase undergoes significant inhibition of activity with increasing concentrations of its substrate, hydroxypyruvic acid phosphate. The enzyme also displays an unusual dual pH optimum. A significant decrease in the $K_i$ for substrate inhibition at pH values corresponding to the valley between these optima is responsible for this phenomena. The change in $K_i$ has an average p$K$ of ~5.8 and involves two functional groups that are protonated and two functional groups that are unprotonated for optimal substrate inhibition to occur. Mutagenesis of positively charged amino acid residues at a putative anion binding site previously revealed by the x-ray structure, produces significant changes in the pH-dependent profile of substrate inhibition. Several single residue mutations eliminate the dual pH optima by reducing substrate inhibition between pH 5 and 7 and a triple mutation was identified that eliminates the substrate inhibition altogether. The mutagenesis data support the conclusion that the anion binding site represents a new allosteric site for the control of enzyme activity and functions in a novel mechanism for substrate inhibition.**

D-3-Phosphoglycerate dehydrogenase (PGDH)[2] (EC 1.1.1.95) from *Mycobacterium tuberculosis* has been shown to differ markedly in structure and activity (1, 2) from the well studied enzyme from *Escherichia coli* (3). Like the *E. coli* enzyme, *M. tuberculosis* PGDH is a homotetramer, but unlike the *E. coli* enzyme, whose subunits are composed of three distinct domains, each *M. tuberculosis* subunit is composed of four distinct domains. The two enzymes have in common a nucleotide binding domain, a substrate binding domain, and a regulatory domain that appear to function similarly in both. The regulatory domains of these enzymes are members of the ACT domain family of small molecule binding regulatory domains (4–6) that bind L-serine, an inhibitor of enzymatic activity. The fourth domain in *M. tuberculosis* PGDH is called the "intervening domain" and is located sequentially between the substrate binding domain and the regulatory domain. The function of this fourth domain in the PGDH subunit is not known but it forms what appears to be a new ligand binding site. This site is a small, solvent accessible pocket surrounded by positively charged amino acid side chains. It was first recognized from the crystal structure where it was observed to bind L-tartrate, a component of the crystallization buffer. Because L-tartrate is found only in plants, and it was present in the buffer in high concentrations, it is unlikely that it is the physiological ligand for this site. Therefore, for simplicity and to avoid ambiguity, we will refer to this site as the "anion binding site" because it appears to be composed completely of cationic side chains.

*E. coli* PGDH exhibits activity with both the physiological substrate, hydroxypyruvic acid phosphate (HPAP), as well as α-ketoglutarate, an analog of HPAP. The *M. tuberculosis* enzyme, on the other hand, displays activity only with HPAP. Furthermore, the *M. tuberculosis* enzyme exhibits significant substrate inhibition characteristics that are not seen with HPAP in the *E. coli* enzyme. Both enzymes utilize NADH as a cofactor and are inhibited in a positively cooperative manner by L-serine. However, the sensitivity of the *M. tuberculosis* enzyme to L-serine inhibition is ~10-fold less than the *E. coli* enzyme, the $IC_{50}$ values being 30 and 3 μM, respectively.

PGDH is an essential enzyme for the *M. tuberculosis* bacteria (7) and may represent a potential target for drug development. The existence of a physiologically relevant inhibitor binding site (for serine) as well as an apparent new ligand binding site of unknown function as part of a new, unique domain provide distinct targets for potential drug interaction. Therefore, it is of considerable interest to better characterize the kinetic and ligand binding characteristics of *M. tuberculosis* PGDH and to explore the potential function of the intervening domain and the anion binding site.

## MATERIALS AND METHODS

HPAP was purchased from Sigma as the dimethylketal tricyclohexylammonium salt and was converted to HPAP according to directions accompanying the reagent. NADH was also purchased from Sigma and all other reagents were analytical grade. The concentration of each HPAP preparation was determined by the amount of NADH converted to $NAD^+$ (8), and was stored in frozen aliquots prior to use. The concentration of HPAP was determined each time the assays were performed. *M. tuberculosis* PGDH concentration was determined by measuring the absorption at 280 nm using an $E_{1\%}$ of 5.6 that was previously determined by amino acid analysis (1). The values

* This work was supported by Grant GM 56676 (to G. A. G.) from the National Institutes of Health. The costs of publication of this article were defrayed in part by the payment of page charges. This article must therefore be hereby marked "*advertisement*" in accordance with 18 U.S.C. Section 1734 solely to indicate this fact.

[1] To whom correspondence should be addressed: Box 8103, WA University School of Medicine, 660 S. Euclid Ave., St. Louis, MO 63110. Tel.: 314-362-3367; Fax: 314-362-4698; E-mail: ggrant@wustl.edu.

[2] The abbreviations used are: PGDH, D-3-phosphoglycerate dehydrogenase; HPAP, hydroxypyruvic acid phosphate (also called phosphohydroxy pyruvate).

for the p$K_a$ of functional groups were calculated using SPARC (ibmlc2.chem.uga.edu/sparc/).

*M. tuberculosis* PGDH activity was measured by following the conversion of NADH to $NAD^+$ by monitoring the decrease in absorbance at 340 nm in the presence of enzyme and HPAP. Assays performed between pH 6.0 and 8.5 were performed in 200 mM potassium phosphate buffer, 1 mM dithiothreitol, 1 mM EDTA at the designated pH and concentrations of NADH and HPAP. Assays performed between pH 4.5 and 5.5 were performed in 200 mM potassium acetate buffer, 1 mM dithiothreitol, 1 mM EDTA. Enzyme concentrations varied between 6 and 16 nM. Enzyme was assayed at pH 6 in both buffers to normalize the enzyme activity at the pH crossover point. No significant difference in relative activity was observed when the addition of KCl was used to maintain an ionic strength of 31 mS/cm across all pH values.

*Expression and Purification—M. tuberculosis* PGDH was expressed as previously described (1). Cells from a 500–1000-ml preparation were re-suspended in 20 mM imidazole, 2 mM dithiothreitol, 1 mM EDTA and brought to pH 6.2 with 0.1 N HCl (buffer A). After a 10-min incubation on ice with 0.16 mg/ml lysozyme, the cells were sonicated for 2–3 min. Crude debris was removed by centrifugation at 12,000 × *g* for 20 min after the addition of 19 mg/ml ammonium sulfate and 35 μl/ml of 10% polyethyleneimine in water. After the addition of 150 mg/ml ammonium sulfate to the supernatant, the cell extract was centrifuged at 12,000 × *g* for 20 min and the supernatant retained. *M. tuberculosis* PGDH was precipitated by the addition of 270 mg/ml ammonium sulfate and the precipitate was collected by centrifugation at 12,000 × *g* for 20 min. The pellet was re-suspended in buffer A and loaded on to a 1.2 × 12-cm column of 5′-ADP-Sepharose, washed with five column volumes of buffer A, and eluted with buffer A containing 200 mM ammonium sulfate and 250 μM NADH. *M. tuberculosis* PGDH was located by assaying for enzymatic activity and appropriate fractions pooled. The 5′-ADP pool was dialyzed against 100 mM potassium phosphate, pH 7.5, 5 mM KCl and loaded onto a 2.6 × 7-cm column of Q-Sepharose. The column was washed with 1 column volume of 100 mM potassium phosphate, pH 7.5, 5 mM KCl and developed with a 1200-ml linear gradient of 100 mM potassium phosphate, pH 7.5, containing 5–1000 mM KCl. *M. tuberculosis* PGDH was located by assaying for enzymatic activity and purity assessed on SDS-PAGE gels.

*Mutagenesis*—Site-specific mutagenesis was performed by standard PCR methods (9). After amplification, the PCR product was digested at appropriate restriction sites flanking the mutated residue and the piece containing the mutation was ligated into the expression vector containing the native enzyme that was digested in the same manner. The sequence of the entire coding region of the protein was determined to be correct by sequencing on an Applied Biosystems 3730 DNA Sequencer. Protein purity was assessed on SDS-PAGE gels and all mutants were present as predominate single bands of the appropriate size. Mutants were isolated as described for the native enzyme.

*Substrate Inhibition*—The kinetic model employed for fitting the data that exhibits substrate inhibition was that described by LiCata and Allewell (10) and utilized the following equation,

$$v = \frac{V_{max} + V_i([S]^x/K_i^x)}{1 + (K^n/[S]^n) + ([S]^x/K_i^x)} \quad \text{(Eq. 1)}$$

where $V_{max}$ and $V_i$ correspond to the catalytic constants $k_{cat}$ and $k_{cat(i)}$ and $n$ is the Hill coefficient. The exponent $x$ is a second Hill coefficient allowing for cooperativity of substrate binding in the inhibitory mode. To obtain convergence for Equation 1, the value of $x$ must be fixed. The integer value for $x$ that gives the best fit was determined empirically.

When there is no cooperativity present, $n$ and $x = 1$. The $V_i$ term describes the case where inhibition is only partial and represents the inhibited velocity. When complete inhibition is observed, $V_i = 0$, and the equation, in the absence of cooperativity, reduces to the standard equation for complete uncompetitive substrate inhibition (11).

$$v = \frac{V_{max}}{1 + (K/[S]) + ([S]/K_i)} \quad \text{(Eq. 2)}$$

*pH Studies*—The pH dependent data were fit to the following equations[3] to determine the p$K_a$ values. The pH dependence of log $V/K$ data were fit to Equation 3,

$$\log(V/K)_{obs} = \log\left(\frac{(V/K)}{1 + ([H]/K_1) + (K_2/[H])}\right) \quad \text{(Eq. 3)}$$

where $V/K$ is the pH independent value and $K_1$ and $K_2$ represent dissociation constants for enzyme or substrate functional groups. The pH dependence of log $(1/K_i)$ data were fit to,

$$\log(1/K_i)_{obs} = \log\left(\frac{\frac{Y_L}{1 + \left(\frac{[H]}{K_1}\right)^2} + Y_H\left(\frac{K_2}{[H]}\right)^2}{1 + \left(\frac{K_2}{[H]}\right)^2}\right) \quad \text{(Eq. 4)}$$

where $Y_L$ and $Y_H$ are pH independent values of $1/K_i$ at low and high pH, respectively, $K_1$ and $K_2$ represent dissociation constants for enzyme or substrate functional groups.

All data were fit with Kaleidograph version 4.0 from Synergy Software. The kinetic parameters listed in Table 1 were derived from at least three determinations.

## RESULTS

*Substrate Inhibition Kinetics*—PGDH from *M. tuberculosis* displays substrate inhibition at high substrate concentrations as shown in Fig. 1. A plot of activity *versus* the log of the substrate concentration (Fig. 1, *inset*) produces a symmetrical curve that approaches complete inhibition at high substrate concentrations. This behavior is consistent with complete uncompetitive substrate inhibition (see below) and the substrate concentration data can be fit well with the equation describing this type of inhibition (Equation 2).

When the HPAP concentration was varied at different fixed concentrations of NADH, the apparent $k_{cat}$ and $K_m$ increase as NADH levels increase. At the same time, the $K_i$ decreases with increasing NADH indicating increasing levels of substrate inhi-

[3] Professor Paul Cook, University of Oklahoma, personal communication.

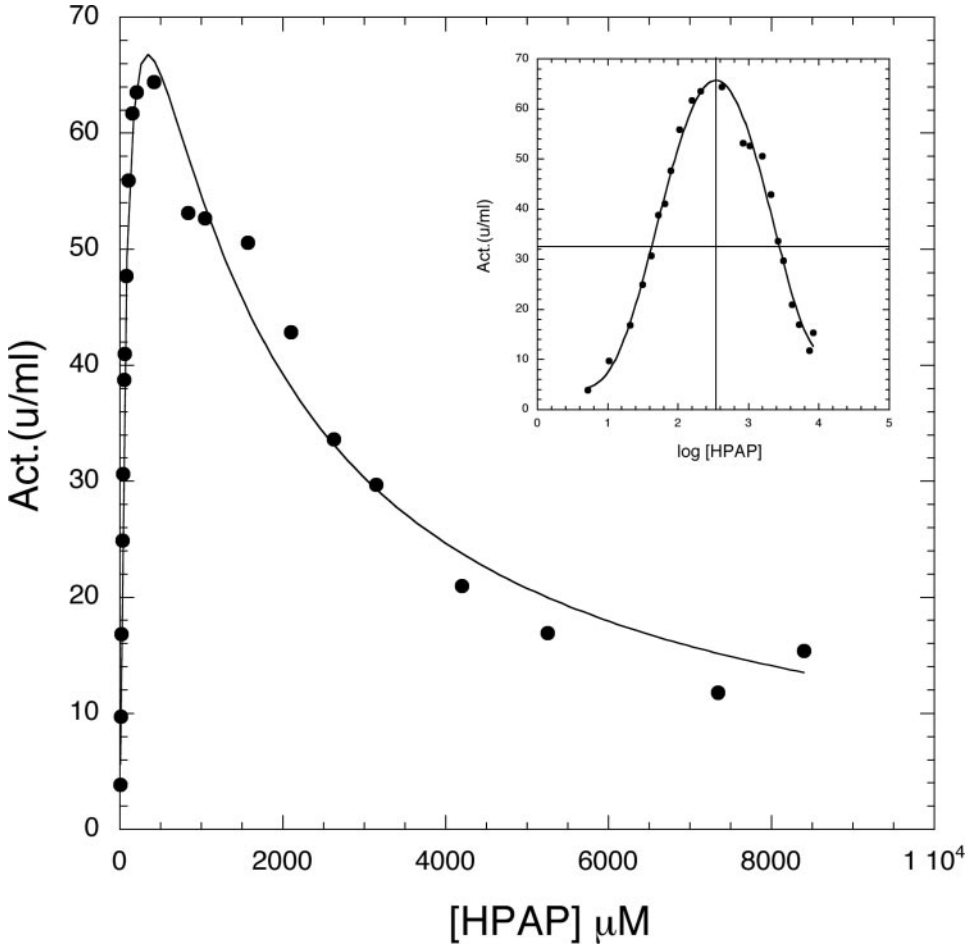


FIGURE 1. **Inhibition of *M. tuberculosis* PGDH by HPAP.** PGDH activity is plotted as a function of HPAP concentration. The *solid line* is a fit to the data (●) using Equation 2. The *inset* is the data plotted as activity *versus* the log of the HPAP concentration. The *lines* are drawn to show the symmetry, with the *vertical line* drawn at the apex of the curve and the *horizontal line* drawn at half-height of the curve.

bition (Fig. 2). Double reciprocol plots of the data display the characteristic non-linear patterns expected for substrate inhibition (12).

Unlike HPAP, NADH does not exhibit substrate inhibition. Rather, a plot of activity *versus* increasing NADH concentrations exhibits a sigmoidal character indicating homotropic positive cooperativity. When the NADH concentration was varied at different fixed concentrations of HPAP, it can be seen that at low HPAP concentrations the maximum velocity of the reaction increases as HPAP increases, but at higher HPAP concentrations this trend was reversed and the velocity of the reaction decreases as the HPAP concentration was increased. This behavior is consistent with uncompetitive substrate inhibition by HPAP (12). The double reciprocal plots for this data are also non-linear due to the homotropic positive cooperativity of NADH.

The crystal structure showing tartrate bound to the enzyme utilized the Na,K salt of tartrate at a concentration of 1 M. However, the inclusion of Na,K tartrate in the assays where HPAP or NADH are varied at a constant level of the other does not seem to have a significant effect on the activity of the enzyme. It may be that whereas tartrate can bind to this site at high concentrations, it may not bind in a productive manner.

*Anion Binding Site*—The anion binding site was originally observed as an area of additional density where two adjacent intervening domains converged. The densities appeared to represent tartrate molecules that were a component of the crystallization buffer (2). The location of the anion binding site at the interfaces of the intervening and regulatory domains is shown in Fig. 3. The tartrate molecules are in hydrogen bonding distances of a group of positively charged residue side chains consisting of His-447 from one subunit and Lys-439′, Arg-451′, and Arg-501′ from the adjacent subunit (′ indicates residues contributed from an adjacent subunit). Arg-501 is actually found in the regulatory domain but extends into this binding pocket. His-447 is found in the strand connecting the regulatory domain and the intervening domain, whereas Lys-439 and Arg-451 are found in the intervening domain. Two molecules of tartrate are bound at each interface because of the symmetry of the structure. This arrangement is similar to the two molecules of serine that bind symmetrically at the regulatory domain interface in *E. coli* PGDH (3). There is an additional cationic side chain, Arg-446, that is found very close to the anion binding site but does not appear to interact with tartrate in the available crystal structure.

The anion binding site was chosen as a focus for site-specific mutagenesis because of the structural similarity of tartrate to the substrate and because only enzymes containing the intervening domain displayed substrate inhibition. The positively charged residues at the anion binding site, His-447, Arg-451′, Arg-501′, Arg-446, and Lys-439′ were converted to alanine side chains by site-directed mutagenesis. A triple mutant where Arg-501′, Arg-451′, and Lys-439′ were all converted to alanine residues was also produced. This combination of residues was chosen because it included all of the residues contributed by one of the subunits at the anion binding site interface. The kinetic parameters, determined at pH 7.5, for these mutations are presented in Table 1. The native enzyme as well as H447A, R451A, and R501A are best fit to Equation 2 and display complete uncompetitive substrate inhibition. The triple mutant was also fit using Equation 2, but displayed little if any apparent substrate inhibition (Fig. 4). On the other hand, R446A and K439A mutations appear to display only partial uncompetitive inhibition as well as cooperative effects and can best be fit with Equation 1. The cooperative effects of the data fit best with $n = 1, x = 2$ for R446A, and $n = 2, x = 2$ for K439A. The $K_m$, $k_{cat}$, and

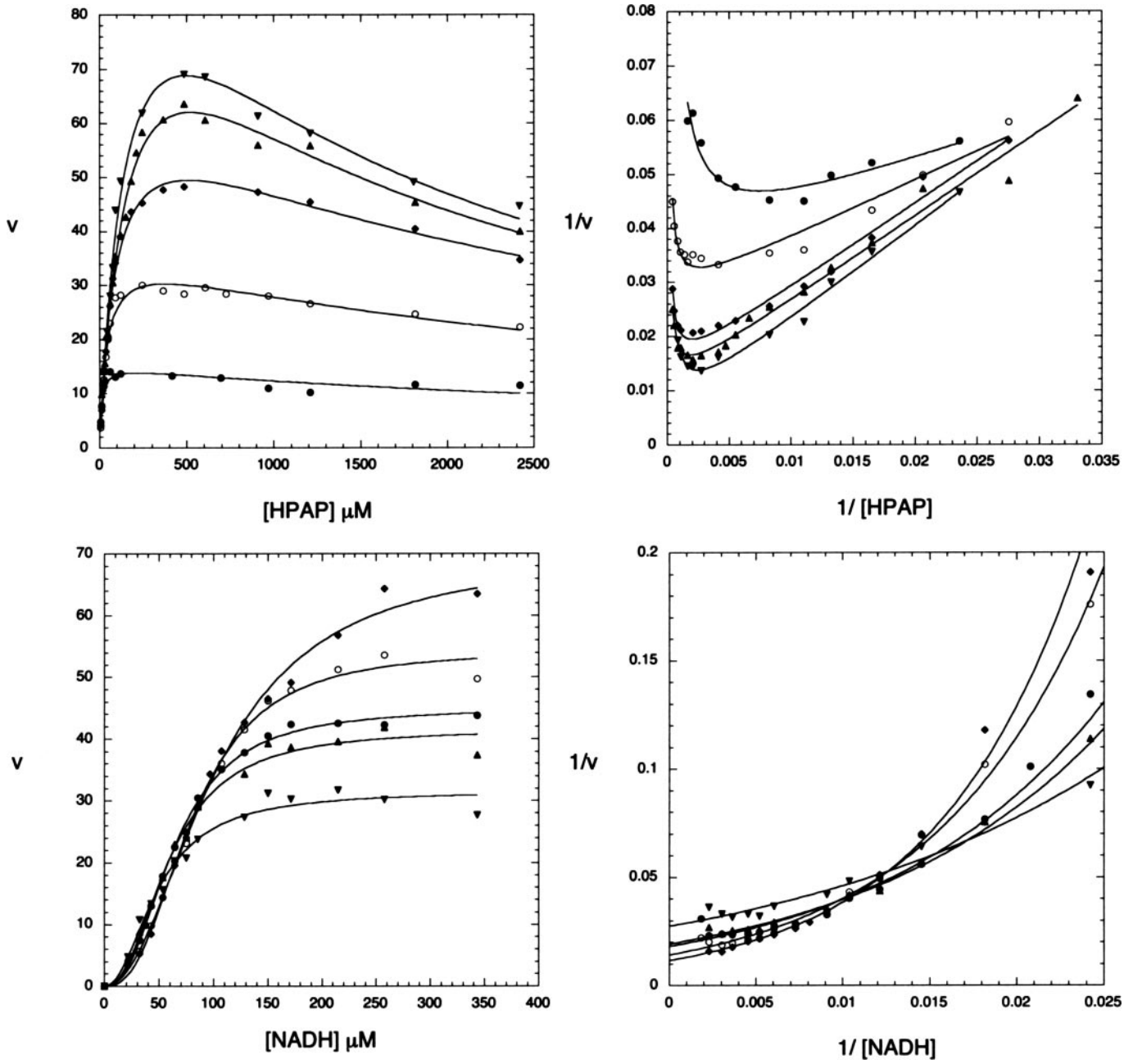


FIGURE 2. **Plots of velocity versus substrate concentration.** The plots on the *left* show the velocity of the enzyme reaction as one substrate is varied at various fixed concentrations of the other substrate. The plots on the *right* are double reciprocal plots of the data on the *left*. *Top*, the HPAP concentration is varied at 50 (●), 100 (○), 180 (◆), 300 (▲), and 500 μM (▼) NADH. *Bottom*, the NADH concentration is varied at 110 (●), 220 (○), 440 (◆), 1760 (▲), and 2640 μM (▼) HPAP.

$K_i$ values for native enzyme and H447A, R451A, R501A, and the triple mutation are comparable, whereas those values for R446A and K439A are significantly reduced. These latter two are also the two mutants that display partial cooperative inhibition.

*Dependence of Activity on pH*—When the pH dependence of the activity of the native enzyme is measured at constant levels of HPAP and NADH, a very unusual dual pH optimum is observed (Fig. 5). The activity is relatively constant between pH 7.5 and 9.5. Above pH 9.5 and below pH 7.5, the activity falls off rapidly. However, at approximately pH 5.7 the activity starts increasing again and reaches a new optimum at approximately pH 5.2 before decreasing once again. The activity of the enzyme was not measured below pH 4.5–5.0 because NADH spontaneously hydrolyzes in this region.

The observation of a dual pH optimum was explored in more detail by determining the kinetic parameters of $K_m$, $k_{cat}$, and $K_i$ at different pH values. The data are presented in Fig. 5 and show that the $K_i$ for substrate inhibition decreases markedly ($1/K_i$ increases) in the area of the valley between the two pH optima. The $k_{cat}$ appears to be essentially pH independent throughout the pH range studied, whereas the $k_{cat}/K_m$ parameter yields p$K$ values of 4.9 and 7.0 when fit to Equation 3. The $1/K_i$ response was relatively sharp between pH 5 and 7 and fitting this data to equation 4 yields p$K$ values

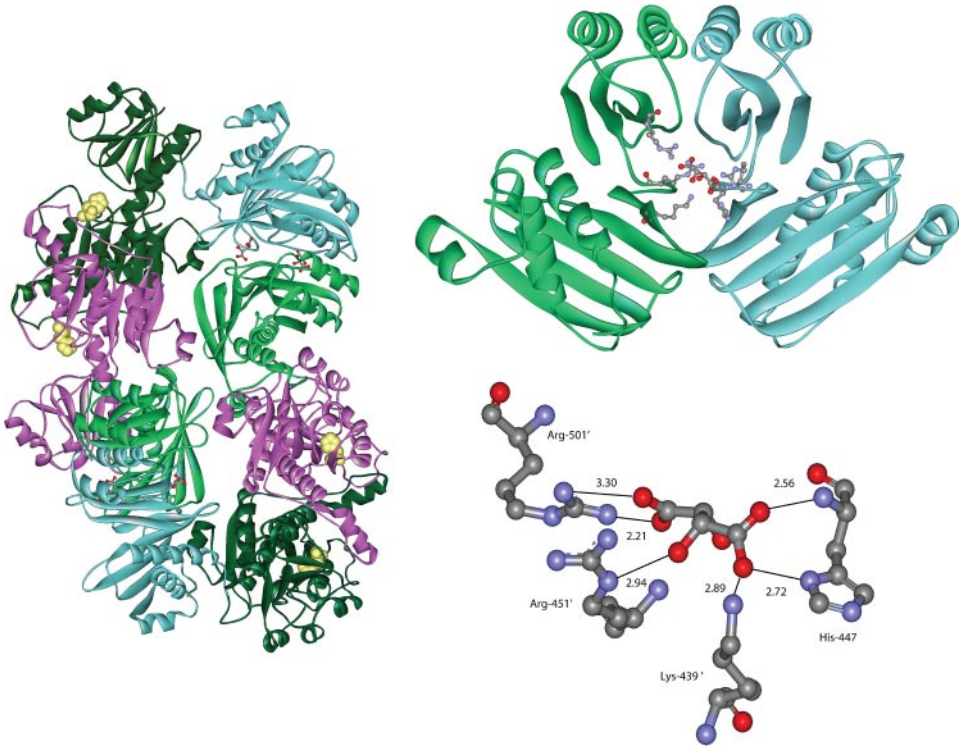


FIGURE 3. ***M. tuberculosis* PGDH and the anion binding site.** *Left*, the structure of the *M. tuberculosis* PGDH homotetramer is depicted as a *ribbon diagram*. The structure contains two subunits per asymmetric unit. One subunit is colored *dark green* and *aqua* (*top* and *bottom*) and the other is colored *purple* and *light green* (*center*). Within the respective subunits, the nucleotide and substrate binding domains together are *dark green* and *purple* and the intervening and regulatory domains together are *light green* and *aqua*. Tartrate molecules are shown in ball-and-stick structure at the anion binding sites. This is best seen in the *upper right-hand* portion of the structure. The active site histidine residues are shown as *yellow* CPK structures. *Upper right*, the location of the anion binding site is shown at the interface between adjacent domains from 2 subunits of *M. tuberculosis* PGDH. The nucleotide and substrate binding domains are not pictured. The subunits are depicted in *green* and *aqua* and correspond to the domains in the *upper right* of the homotetramer looking along the domain interface. The tartrate molecule and the amino acid residue side chains forming hydrogen bonds with it are shown in ball-and-stick representation (oxygens are colored *red*, nitrogens are *blue*, and carbons are *gray*). The regulatory or ACT domains are the $\beta\alpha\beta\beta\alpha\beta$ structures at the *top* of the figure and the intervening domains are toward the *bottom* of the figure. Only a single tartrate is depicted for clarity at the front of the structure. Because of the symmetry of the interface, a second tartrate molecule, which is not shown, binds in a similar manner toward the back of the structure (see Protein Data Bank code 1YGY). *Lower right*, the tartrate molecule forms hydrogen bonds with residues Arg-501, Arg-451, Lys-439, and His-447′. Hydrogen bonds are shown with *solid lines* and the distances are given in Angstroms.

**TABLE 1**

**Kinetic parameters of native and mutated *M. tuberculosis* D-3-phosphoglycerate dehydrogenase**

| Enzyme | $K_m$ | $k_{cat}$ | $K_i$ | $k_{cat}/K_m$ |
|---|---|---|---|---|
| | $\mu M$ | $s^{-1}$ | $\mu M$ | $M^{-1}\,s^{-1}$ |
| Native | 170 ± 50 | 2461 ± 281 | 950 ± 120 | $1.5 \times 10^7$ |
| H447A[a] | 160 ± 10 | 1446 ± 191 | 870 ± 50 | $0.9 \times 10^7$ |
| R451A[a] | 190 ± 40 | 1881 ± 109 | 950 ± 150 | $1.0 \times 10^7$ |
| R501A[a] | 180 ± 10 | 1989 ± 88 | 1020 ± 30 | $1.1 \times 10^7$ |
| R446A[b] | 123 ± 18 | 467 ± 49 | 289 ± 15 | $0.4 \times 10^7$ |
| K439A[c] | 75 ± 1 | 368 ± 38 | 54 ± 4 | $0.5 \times 10^7$ |
| R501A, R451A, K439A[a] | 243 ± 16 | 1558 ± 58 | 7218 ± 1379 | $0.6 \times 10^7$ |

[a] Fit to Equation 2.
[b] Fit to Equation 1 with $n = 1, x = 2$.
[c] Fit to Equation 1 with $n = 2, x = 2$.

of 5.78 and 5.84. Because these values are indistinguishable within error, they are considered to be a single p$K$ of 5.8.

The anion binding site mutant enzymes did not all produce the same dual pH optima observed for the native enzyme (representative plots are shown in Fig. 6). Instead, H447A and R501A exhibited a single broad bell-shaped curve with an acidic side p$K$ of ~4.8. R446A and R451A yielded similar profiles. However, a slight shoulder was visible at a pH corresponding to the valley observed for the native enzyme. The triple mutation also exhibited a single broad pH profile, but it appeared to be shifted by ~0.5–1 pH units to the acid side. K439A retained the dual optima of the native enzyme but with a broadened valley that corresponded to p$K$ values of ~4.9 and 8.0 as compared with 4.9 and 7.0 for the native enzyme. When the pH-dependent kinetic parameters are determined for H447A and R501A, the decrease in $K_i$ between pH 5 and 7 is absent or greatly reduced. A comparison of the $1/K_i$ values for native, H447A, R501A, and K4539A PGDH is shown in Fig. 7. The $K_i$ values for R501A are relatively constant at all pH values studied and the substrate inhibition profiles exhibit apparent complete inhibition. The same is true for H447A from pH 7.5 to 6.0. However, below pH 6.0 the inhibition profile changes from that of complete inhibition to partial inhibition at pH 5.5 and no apparent substrate inhibition at pH 5.0. An increase in substrate inhibition, similar to the native enzyme, is apparent for K439A. In this case, substrate inhibition is partial from pH 8.5 to 5.5, and then reverts to a low level of complete inhibition at pH 5.0. The $1/K_i$ values are elevated at pH values that display a reduced velocity in the valley between the two apparent pH optima. Furthermore, the data demonstrate that there is a correlation between the widened valley seen for K439A, pH 5.5–7.5, compared with native enzyme, pH 5.5–6.5, and the pH specific increase in the $1/K_i$ values for that mutant.

## DISCUSSION

The activity of *M. tuberculosis* PGDH exhibits substrate inhibition at high concentrations of the substrate HPAP. This is similar to what was reported for rat PGDH (13), which also possesses an intervening domain, but is not seen in the *E. coli* enzyme that lacks an intervening domain. This suggested that the intervening domain was potentially involved in the mechanism of substrate inhibition.

Surprisingly, analysis of the pH dependence of the activity of *M. tuberculosis* PGDH produces a very unusual but distinct dual pH optimum profile for this enzyme. Subsequent analysis of the kinetic parameters demonstrates that whereas the $k_{cat}$ is relatively independent of pH, the substrate inhibi-

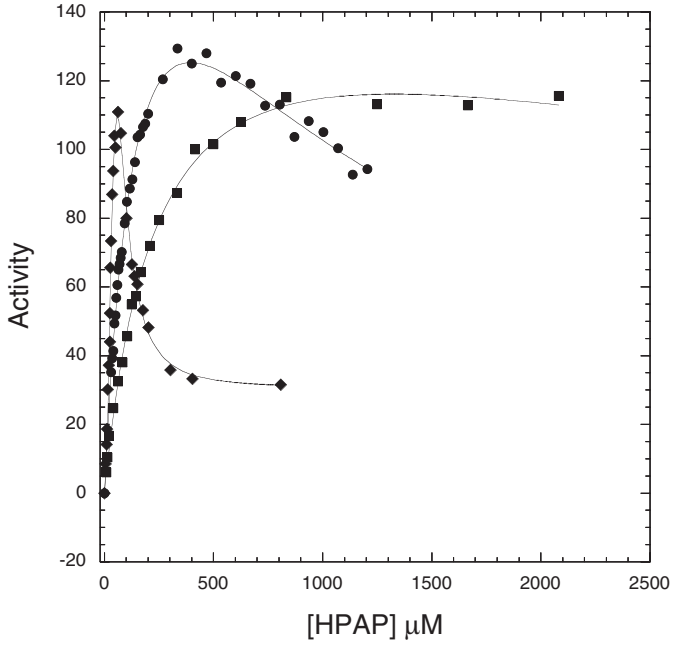


FIGURE 4. **Comparison of inhibition patterns.** Enzyme activity is plotted *versus* HPAP concentration for K439A (◆), native PGDH (●), and R501A,R451A,K439A (■). The data for K439A is fit to Equation 1 and that for native PGDH and the triple mutant fit to Equation 2.

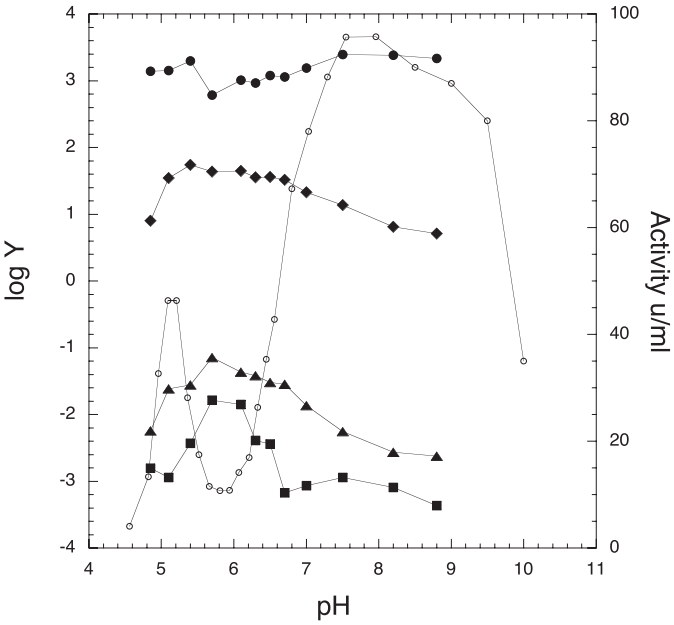


FIGURE 5. **Enzyme activity and kinetic parameters as a function of pH.** The enzyme activity and the log of the kinetic parameters (log *Y*) are plotted as a function of pH. The activity of wild-type *M. tuberculosis* PGDH (○) and log $k_{cat}$ (●), log $k_{cat}/K_m$ (◆), log $1/K_m$ (▲), and log $1/K_i$ (■).

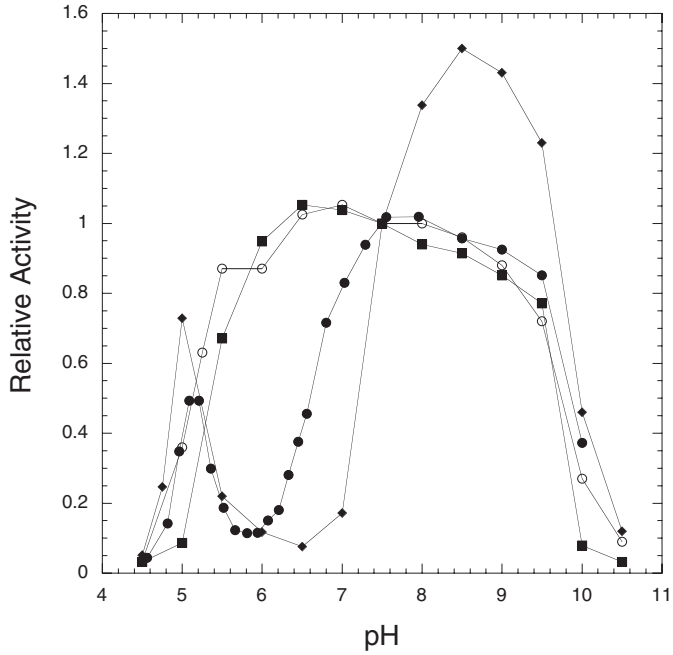


FIGURE 6. **pH dependence of activity for representative enzymes.** Relative activity is plotted *versus* pH. The plots are normalized by setting the value at pH 7.5 to 1. Wild-type *M. tuberculosis* PGDH (●), H447A (■), R446A (○), and K439A (◆).

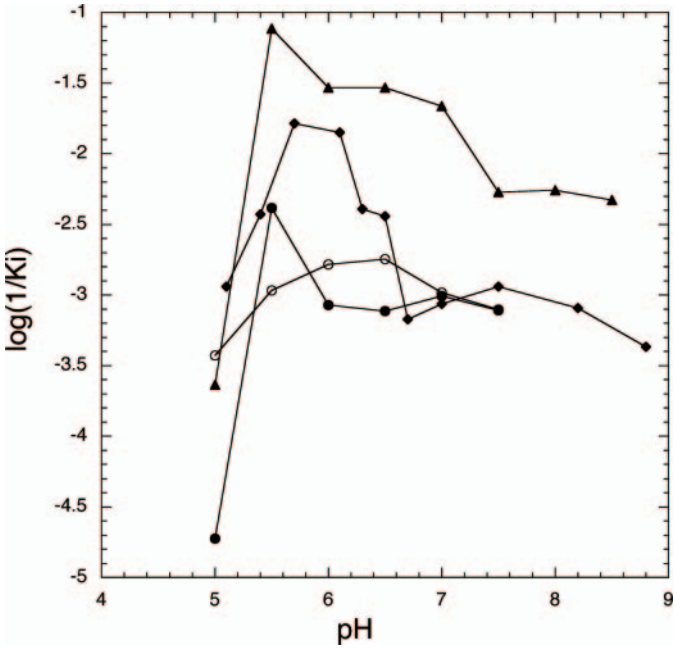


FIGURE 7. **Log of $1/K_i$ as a function of pH.** The log of $1/K_i$ is plotted as a function of pH for wild-type *M. tuberculosis* PGDH (◆), K439A (▲), H447A (●), and R501A (○).

tion of enzymatic activity actually increases significantly in the area between the pH optima. This rise and then drop in substrate inhibition as the pH is lowered appears to be responsible for the apparent dual optima that is observed when the enzyme is assayed at a single constant concentration of substrate and cofactor. Subsequent investigation of the potential function of the anion binding site by site-directed mutagenesis revealed a correlation between the unusual dual pH optimum observed for this enzyme and the potential involvement of this site in the substrate inhibition characteristics of the enzyme.

As originally pointed out (2), tartrate is most likely not the physiological ligand for this site because, as far as we know, it is found only in plants. Furthermore, tartrate does not seem to affect catalytic activity in *in vitro* assays. Although tartrate has some similarity to the substrate, hydroxypyruvic acid phosphate, in that both possess anionic groups at either end of their carbon chains, hydroxypyruvic acid phosphate is larger than

tartrate and possesses an ionizable phosphate group in place of one of the carboxyl groups of tartrate. Thus, the interaction of hydroxypyruvic acid phosphate at this site could be more extensive than that seen for tartrate. The reason that tartrate does not appear to produce inhibition could be due to an unproductive binding mode because it is lacking the phosphate group that provides for a more elongated molecule, a higher charge density, and a higher p*K*. Furthermore, binding of substrate may potentially involve additional interactions with the protein, such as with Arg-446 that displays a definite effect on the substrate inhibition but is not observed to be interacting with tartrate in the crystal structure.

A fit of the log $k_{cat}/K_m$ values of the native enzyme at various pH values to Equation 3 yields p*K* values of ~7.0 and 4.9. When an increase in substrate inhibition is absent, as in H447A and R501A, a single p*K* of ~4.9 is observed. The p*K* of 4.9 probably represents a group at the active site being protonated that is required in its unprotonated state for activity. This may represent His-280, which forms a His-Glu pair with Glu-262 at the active site. The apparent p*K* of 7.0 appears to result as a function of the increase in substrate inhibition.

The fit of the log $1/K_i$ plot as a function of pH, for the native enzyme, to Equation 4, yields two p*K* of ~5.8 that are indistinguishable within error. This peak is well defined and clearly shows a slope of ~2 on either side. This indicates that two functional groups are protonated and two functional groups are unprotonated for optimal substrate inhibition to occur. These groups could be on either the protein or the substrate and the value of 5.8 represents an average $pK_a$ of the groups involved. It seems likely that His-447 at the anion binding site and the phosphate group of the substrate are involved, potentially in a charge interaction. As the pH decreases, both groups, which have a normal $pK_a$ of ~6, would become increasingly protonated. This would increase the positive charge on the histidine but at the same time decrease the negative charge on the phosphate group. These opposing phenomena would tend to produce the strongest charge interaction at their $pK_a$ where the relative concentration of the salt bridge would be the highest. This corresponds to the $pK_a$ of the increase in substrate inhibition. Other potential groups that could be involved are the carboxyl group of the substrate ($pK_a$ = 3.3) and Lys-439 on the protein ($pK_a$ = 9.7) if their pK values were sufficiently perturbed by the local environment. The average $pK_a$ of these groups is close to the $pK_a$ of substrate inhibition. Involvement of protonation of the arginine residues at the anion binding site seems unlikely due to the very large perturbation of their normal $pK_a$ values ($pK_a$ = 12) that would be required.

When either Arg-501 or His-447 are mutated to alanine residues, the dual pH optimum and the decrease in $K_i$ are no longer observable. Mutation of Arg-446 and Arg-451 produces a similar result although a slight shoulder is still observed at this point in the pH curve. Because these residues are found on adjacent subunits, the binding of substrate may serve to bridge the adjacent subunits through a hydrogen bond or charge interaction network. The substrate inhibition would be more pronounced at lower pH due to the increased formation of salt bridges between the substrate and the residues at the anion binding site, as discussed above. These salt bridges would be expected to be stronger than non-ionic hydrogen bonds.

Mutation of Lys-439, on the other hand, not only maintains the dual pH optimum, but actually increases its range from pH 5–7 to 5–8. Consistent with this, the range over which the $K_i$ decreases ($1/K_i$ increases) for this mutant is also increased by the same extent. Furthermore, the mutation K439A, as well as R446A, changes the nature of the substrate inhibition from complete inhibition to partial inhibition, thus defining their role in contributing to the extent of inhibition.

H447A and R501A mutants still exhibit substrate inhibition between pH 5 and 7 comparable in magnitude to that seen above pH 7 for the native enzyme. On the other hand, the triple mutant, R501A,R451A,K439A, which eliminates all of the residues from one subunit, displays a nearly complete loss of substrate inhibition at all pH values.

Although the kinetic data are consistent with classical uncompetitive substrate inhibition, where the second substrate (HPAP) binds to the active site prior to release of the product of the other substrate (NAD), the mutagenesis data strongly support the involvement of the anion binding site in the substrate inhibition mechanism. This is particularly apparent with the almost complete loss of substrate inhibition seen with the triple mutant. This, along with the observation that substrate inhibition has only been seen in those PGDH enzymes containing intervening domains, provides strong support for a mechanism of substrate inhibition caused by substrate binding at a second site away from the active site.

The internal pH of the *M. tuberculosis* bacteria is not well characterized. If the cytosolic pH of actively growing *M. tuberculosis* is close to neutrality, as one might expect, the observed increase in $K_i$ at lower pH may not be physiologically relevant to the actively growing bacteria. However, this phenomenon may be relevant to the persistent phase of the bacteria. After the initial infection of macrophages in the lung, the immune response of the host develops granulomas or "tubercles" around the infection resulting in a latent, persistent stage of infection. Phagosomes containing viable *M. tuberculosis* equilibrate to a pH of ~6.2 (14, 15) that causes them to be retained within the endosomal pathway and isolates the bacterium from the degradative environment of the lysosome. This is within the optimum pH range of 5.7–6.2 of the pH-dependent increase in substrate inhibition reported here for *M. tuberculosis* PGDH. This coincidence suggests that there may be some connection between the persistent state of *M. tuberculosis* infection and a need to restrict the activity of this metabolic enzyme. However, this hypothesis would depend on whether or not the cytosolic pH of the bacteria assumes the pH of its environment in the tubercule.

Like *E. coli* PGDH, *M. tuberculosis* PGDH is feedback regulated by L-serine, the immediate end product of its pathway. These studies support an additional allosteric mechanism of inhibition of PGDH activity through interaction of substrate with the anion binding site of the enzyme. This has interesting mechanistic implications for the regulation of enzyme activity and for the function of the unique intervening domain found in D-3-phosphoglycerate dehydrogenase from *M. tuberculosis* and

perhaps other species. The anion binding site also provides a potential new target for drug development.

*Acknowledgments—We thank Dr. James C. Sacchettini and Dr. Paul Cook for helpful comments.*

## REFERENCES


1. Dey, S., Hu, Z., Xu, X. L., Sacchettini, J. C., and Grant, G. A. (2005) *J. Biol. Chem.* **280,** 14884–14891
2. Dey, S., Grant, G. A., and Sacchettini, J. C. (2005) *J. Biol. Chem.* **280,** 14892–14899
3. Schuller, D., Grant, G. A., and Banaszak, L. (1995) *Nat. Struct. Biol.* **2,** 69–76
4. Aravind, L., and Koonin, E. V. (1999) *J. Mol. Biol.* **287,** 1023–1040
5. Chipman, D. M., and Shaanan, B. (2001) *Curr. Opin. Struct. Biol.* **11,** 694–700
6. Grant, G. A. (2006) *J. Biol. Chem.* **281,** 33825–33829
7. Sassetti, C. M., Boyd, D. H., and Rubin, E. J. (2003) *Mol. Microbiol.* **48,** 77–84
8. Sugimoto, E., and Pizer, L. I. (1968) *J. Biol. Chem.* **243,** 2081
9. Cormack, B. (1991) in *Current Protocols in Molecular Biology* (Ausubel, F. M., Brent, R., Kingston, R. E., Moore, D. D., Seidman, J. G., Smith, J. A., and Struhl, K., eds) pp. 8.5.1–8.5.9, John Wiley and Sons, New York
10. LiCata, V. J., and Allewell, N. M. (1997) *Biophys. Chem.* **64,** 225–234
11. Cleland, W. (1979) *Methods Enzymol.* **63,** 500–513
12. Segel, I. H. (1975) *Enzyme Kinetics*, pp. 818–826, Wiley Interscience, New York
13. Achouri, Y., Rider, M. H., Van Schaftingen, E., and Robbi, M. (1997) *Biochem. J.* **323,** 365–370
14. Russell, D. G. (2007) *Nat. Rev. Microbiol.* **5,** 39–47
15. Honer zu Bentrup, K., and Russell, D. G. (2001) *Trends Microbiol.* **9,** 597–605